

Weak-measurement-induced asymmetric dephasing: manifestation of intrinsic measurement chirality

Kyrylo Snizhko,^{1,2} Parveen Kumar,¹ Nihal Rao,^{1,3,4} and Yuval Gefen¹

¹*Department of Condensed Matter Physics, Weizmann Institute of Science, Rehovot, 76100 Israel*

²*Institute for Quantum Materials and Technologies,*

Karlsruhe Institute of Technology, 76021 Karlsruhe, Germany

³*Present affiliation: Arnold Sommerfeld Center for Theoretical Physics,*

University of Munich, Theresienstr. 37, 80333 München, Germany

⁴*Present affiliation: Munich Center for Quantum Science and Technology (MCQST), Schellingstr. 4, 80799 München, Germany*

Geometrical dephasing is distinct from dynamical dephasing in that it depends on the trajectory traversed, hence it reverses its sign upon flipping the direction in which the path is traced. Here we study sequences of generalized (weak) measurements that steer a system in a closed trajectory. The readout process is marked by fluctuations, giving rise to dephasing. Rather than classifying the latter as “dynamical” and “geometrical”, we identify a contribution which is invariant under reversing the sequence ordering and, in analogy with geometrical dephasing, one which flips its sign upon the reversal of the winding direction, possibly resulting in partial suppression of dephasing (i.e., “coherency enhancement”). This dephasing asymmetry (under winding reversal) is a manifestation of intrinsic chirality, which weak measurements can (and generically do) possess. Furthermore, the dephasing diverges at certain protocol parameters, marking topological transitions in the measurement-induced phase factor.

Dephasing is a ubiquitous feature of open quantum systems [1, 2]. Undermining coherency, it facilitates the crossover to classical behavior, and comprises a fundamental facet of the dynamics of mesoscopic systems [3–10]. Dephasing has to be taken into account when designing mesoscopic devices [11, 12], specifically those directed at quantum information processing [1, 13–15].

A particularly intriguing type of dephasing appears when geometrical phases [16, 17] emerge in open quantum systems [18–25]. On top of conventional dynamical dephasing (arising due to the fluctuations of the system’s energy and proportional to the evolution time), Refs. [24–26] found a geometrical contribution to dephasing. Such geometrical dephasing (GD) has two salient features. First, it can be expressed through an integral of the underlying Berry curvature [27, 28]. Second, similarly to Hamiltonian-generated geometrical phase, GD flips its sign upon the reversal of the evolution protocol (the directionality in which the closed path is traversed). The existence of geometrical dephasing has been confirmed experimentally [29]. Recent theoretical studies [27, 28] have generalized GD to the case of non-Abelian phases.

On a seemingly unrelated front, measurement-induced geometrical phases have recently become an object of both experimental [30] and theoretical [31] interest. Notably, measurement in quantum mechanics involves stochasticity. It is thus natural to ask whether dephasing emerges in measurement-based protocols [32] and to investigate its relation to Hamiltonian-induced dephasing [33].

The challenge of the present paper is two-fold. We first ask whether weak-measurement-induced phases go hand-in-hand with emergent dephasing. Secondly, provided that dephasing is part of such protocols, does this

dephasing have a term similar to GD? Our main findings are: (i) Indeed, measurement-induced generation of phases does give rise to dephasing. (ii) In similitude to Hamiltonian dynamics of dissipative systems, leading to dynamical and geometrical components, here both the phase and the dephasing generated by measurement protocols comprise a symmetric and an antisymmetric (w.r.t. changing directionality) components. The latter manifests the existence of intrinsic chirality in weak measurements (cf. Fig. 1). (iii) The emergent dephasing in such measurement-based steering protocols may diverge. These divergences are associated with topological transitions underlying the steering protocols.

Measurement model.—As a concrete (but generalizable) example we consider a spin-1/2 system subject to non-projective measurements. Our detector is a two-level quantum object, its states labeled as $r = 0, 1$. The measurement procedure comprises coupling the detector to the system, decoupling it, and then measuring the detector projectively in the $|r\rangle$ basis. The system evolution under measurement can be described as $|\psi\rangle \rightarrow \mathcal{M}^{(r)}|\psi\rangle$ [34–36] where $\mathcal{M}^{(r)}$ is the generalized measurement operator (also known as the Kraus operator) associated with the readout $r = 0/1$.

Resorting to a protocol where we are blind to the detector readouts (i.e., tracing out the detector), the measurement is indistinguishable from a (carefully engineered) Markovian environment. However, as we shall see in the coming sections, a non-conventional “two-replica” averaging over measurement readouts is important for the effects reported here.

Depending on the system-detector coupling, the measurement back-action may vary. We focus on the specific

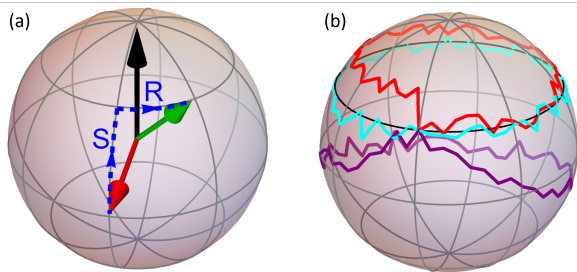


Figure 1. Measurement-induced trajectories. (a)—The back-action of a generalized measurement. Under a projective measurement yielding readout $r = 0$, the system’s initial state (red arrow) would become $|\uparrow\rangle$ (black arrow). For finite measurement strength, the state is only pulled towards $|\uparrow\rangle$ and also rotated around the z axis (green arrow). These two back-action aspects (illustrated by dashed blue lines) are quantified by parameters S and R in Eq. (2). The direction of the rotation (the sign of R) sets the measurement’s chirality. (b)—Schematic illustration of trajectories induced by a sequence of measurements along some parallel (black line). Depending on the sequence of readouts $\{r_k\}$, different trajectories (red, cyan, purple) and different phases $\chi_{\{r_k\}}^{(d)}$ are induced.

case with $\mathcal{M}_{\mathbf{n}}^{(r)} = U^{-1}(\mathbf{n})M^{(r)}U(\mathbf{n})$, where

$$U(\mathbf{n}) = \begin{pmatrix} \cos \frac{\theta}{2} & \sin \frac{\theta}{2} e^{-i\varphi} \\ \sin \frac{\theta}{2} & -\cos \frac{\theta}{2} e^{-i\varphi} \end{pmatrix}, \quad (1)$$

$$M^{(0)} = \begin{pmatrix} 1 & 0 \\ 0 & e^{-S-iR} \end{pmatrix}, \quad M^{(1)} = \begin{pmatrix} 0 & 0 \\ 0 & \sqrt{1-e^{-2S}} \end{pmatrix}, \quad (2)$$

with (θ, φ) being the spherical angles specifying the measured spin direction \mathbf{n} .

The effect of such measurements is illustrated in Fig. 1(a). Upon reading out $r = 0$, the spin is pulled toward direction \mathbf{n} (at strength S), and is rotated around it (cf. the parameter R) [37]. In conventional measurement models, this rotation is disregarded. However, it can exist in practice, and, as is shown below, it plays a crucial role in the behavior of measurement-induced phases and dephasing. In particular, the sign of R determines the measurement’s chirality. The readout $r = 1$ results in the spin being *projected* onto direction $-\mathbf{n}$. The measurement strength S determines the probability $p_r = \langle \psi | \mathcal{M}_{\mathbf{n}}^{(r)\dagger} \mathcal{M}_{\mathbf{n}}^{(r)} | \psi \rangle$ of this event. For a vanishing measurement strength, $S = 0$, the readout $r = 1$ never occurs. The standard projective measurement is recovered for $S \rightarrow \infty$. Note that in the limit of a projective measurement R has no effect, which is why the effect of measurement chirality has been overlooked so far.

The protocol.—Details of our protocol are inspired by studies of dynamical quantum Zeno effect, cf. Ref. [38], where a spin-1/2 system is prepared in the direction $\mathbf{n}_0 = (\sin \theta, 0, \cos \theta)$ and then subjected to a sequence of $N + 1$ projective measurements corresponding to directions

$\mathbf{n}_k = (\sin \theta \cos \varphi_k, \sin \theta \sin \varphi_k, \cos \theta)$, $\varphi_k = 2\pi kd/(N+1)$. Here $d = \pm 1$ defines the directionality of the trajectory. When $N \rightarrow \infty$, the spin state follows the measurement directions with probability 1 and acquires the geometric Pancharatnam phase $-\pi d(1 - \cos \theta)$.

We employ the same protocol for inducing phases by measurements, but with the first N measurements being non-projective, as defined in Eqs. (1–2) with $S = 2C/N$ and $R = 2A/N$. The parameters C and A (of $O(1)$) characterize the measurement; the $1/N$ scaling is required in order to avoid the quantum Zeno effect in the $N \rightarrow \infty$ limit, allowing for non-trivial evolution of the system’s trajectory and the study of measurement chirality. With this modification, the spin state follows a trajectory parameterized by the readout sequence $\{r_k\}$, cf. Fig. 1(b) (each sequence is associated with a specific probability). We keep the final measurement, $k = N + 1$, projective, and postselect it on yielding $r = 0$ readout in order to ensure that the spin has followed a closed trajectory on the Bloch sphere.

The observable.—For each readout sequence $\{r_k\}$, the spin state acquires a phase $\chi_{\{r_k\}}^{(d)}$. After averaging over different readout sequences, we define the averaged phase, $\bar{\chi}^{(d)}$, and the dephasing parameter, $\alpha^{(d)}$, through

$$\langle e^{2i\chi_{\{r_k\}}^{(d)}} \rangle_{\{r_k\}} = e^{2i\bar{\chi}^{(d)} - \alpha^{(d)}}. \quad (3)$$

This somewhat arbitrary form of averaging in Eq. (3) is motivated by the following proposal for observing the measurement-induced phases [31, 39]. The phase could, naively, be measured by an interference experiment, where a “flying spin-1/2”, represented by an impinging electron, is split between two arms and subjected to measurements in one of them. Such a protocol, however, presents the following problem: the detector changing its state would not only induce a back-action on the system (the flying spin-1/2), but would also constitute a “which-path” measurement, undermining the interference, just as conventional coupling to the environment would. Instead, one can resort to a measurement setup where each detector is coupled to respective points on both arms. The system-detector couplings are engineered such that the phases accumulated in the respective arms are $\chi_{\{r_k\}}^{(d)}$ and $-\chi_{\{r_k\}}^{(d)}$ for each and every sequence of readouts $\{r_k\}$. With these designed couplings, the probabilities of obtaining a specific readout sequence $\{r_k\}$ are identical for both arms, hence, no “which path” measurement. The interference pattern then corresponds to the relative phase $e^{2i\chi_{\{r_k\}}^{(d)}}$ and is averaged over runs with different readout sequences $\{r_k\}$.

Derivation of the dephasing factor.—The phase accumulated under a sequence of measurements can be calculated as follows. Denote the initial system state $|\psi_0\rangle = \cos \frac{\theta}{2} |\uparrow\rangle + \sin \frac{\theta}{2} |\downarrow\rangle$. After performing the sequence of N generalized measurements, for

a given readout sequence $\{r_k\} = \{r_1, \dots, r_N\}$, the system state becomes $\mathcal{M}_{\mathbf{n}_N}^{(r_N)} \dots \mathcal{M}_{\mathbf{n}_2}^{(r_2)} \mathcal{M}_{\mathbf{n}_1}^{(r_1)} |\psi_0\rangle$. The last projective measurement makes the system state $|\psi_0\rangle \langle \psi_0| \mathcal{M}_{\mathbf{n}_N}^{(r_N)} \dots \mathcal{M}_{\mathbf{n}_1}^{(r_1)} |\psi_0\rangle$. The matrix element

$$\langle \psi_0 | \mathcal{M}_{\mathbf{n}_N}^{(r_N)} \dots \mathcal{M}_{\mathbf{n}_1}^{(r_1)} | \psi_0 \rangle = \sqrt{P_{\{r_k\}}^{(d)}} e^{i\bar{\chi}_{\{r_k\}}^{(d)}} \quad (4)$$

defines the measurement-induced phase $\bar{\chi}_{\{r_k\}}^{(d)}$ and the probability $P_{\{r_k\}}^{(d)}$ of obtaining readout sequence $\{r_k\}$ (including $r = 0$ for the last *projective* measurement, bringing the system to $|\psi_0\rangle$). Considering all possible measurement readout sequences $\{r_k\}$, the averaged phase $\bar{\chi}^{(d)}$

and the dephasing parameter $\alpha^{(d)}$ are given by

$$e^{2i\bar{\chi}^{(d)} - \alpha^{(d)}} = \sum_{\{r_k\}} \left(\langle \psi_0 | \mathcal{M}_{\mathbf{n}_N}^{(r_N)} \dots \mathcal{M}_{\mathbf{n}_1}^{(r_1)} | \psi_0 \rangle \right)^2 = \sum_{\{r_k\}} P_{\{r_k\}}^{(d)} e^{2i\bar{\chi}_{\{r_k\}}^{(d)}}. \quad (5)$$

We compute $e^{2i\bar{\chi}^{(d)} - \alpha^{(d)}}$ using the following trick. Note that $\langle \psi_0 | \mathcal{M}_{\mathbf{n}_N}^{(r_N)} \dots \mathcal{M}_{\mathbf{n}_1}^{(r_1)} | \psi_0 \rangle = \langle \uparrow | \delta U M^{(r_N)} \delta U \dots \delta U M^{(r_1)} \delta U | \uparrow \rangle$, where $\delta U = U(\mathbf{n}_{k+1})U^{-1}(\mathbf{n}_k)$ is a matrix that does not depend on k , cf. Eqs. (1-2). In order to calculate the sum over $\{r_k\}$, we define a matrix $\mathfrak{M}_{s_1 s_2}^{s'_1 s'_2} = \sum_r \langle s'_1 | M^{(r)} \delta R | s_1 \rangle \langle s'_2 | M^{(r)} \delta R | s_2 \rangle$. Here s_i (“before the measurement”) and s'_i (“after the measurement”) take values \uparrow / \downarrow with $i = 1, 2$ being the replica index. We find that for $N \rightarrow \infty$

$$\mathfrak{M} = \mathbb{I} + \Lambda/N + O(N^{-2}), \quad (6)$$

where Λ is a constant matrix that depends on the measurement parameters C and A , polar angle θ , and directionality d , characterizing the protocol:

$$\Lambda = \begin{pmatrix} 2i\pi d \cos \theta & -i\pi d \sin \theta & -i\pi d \sin \theta & 0 \\ -i\pi d \sin \theta & -2(C + iA) & 0 & -i\pi d \sin \theta \\ -i\pi d \sin \theta & 0 & -2(C + iA) & -i\pi d \sin \theta \\ 0 & -i\pi d \sin \theta & -i\pi d \sin \theta & -2i\pi d \cos \theta - 4iA \end{pmatrix} \begin{bmatrix} \uparrow\uparrow \\ \uparrow\downarrow \\ \downarrow\uparrow \\ \downarrow\downarrow \end{bmatrix}. \quad (7)$$

Then

$$e^{2i\bar{\chi}^{(d)} - \alpha^{(d)}} = \lim_{N \rightarrow \infty} (\mathfrak{M}^N)_{\uparrow\uparrow}^{\uparrow\uparrow} = [\exp(\Lambda)]_{\uparrow\uparrow}^{\uparrow\uparrow}. \quad (8)$$

Classification of dephasing.—In light of Eq. (8), it is tempting to denote $\alpha^{(d)}$ and $\bar{\chi}^{(d)}$ geometrical since they do not depend on the protocol duration (number of measurements). Such an identification would be erroneous, as can be easily seen from the following argument: For $C = 0$ (equivalently, $S = 0$ in Eq. (2)), our measurement-induced evolution is equivalent to *non-adiabatic* Hamiltonian evolution (readout $r = 1$ never occurs; the back-action with the Kraus operator $\mathcal{M}_{\mathbf{n}}^{(0)}$ is equivalent to a Hamiltonian rotation). While the accumulated phase in that case does not scale with N , it is known that it admits a non-trivial separation into the dynamical and geometrical components [40, 41]. At the same time, these dynamical and geometrical components behave non-trivially with respect to directionality reversal, $d \rightarrow -d$, which hinders a simple classification based on symmetry properties. Here we do not delve deeper into this classification issue [42] but rather focus on the behavior of dephasing and the measurement-induced phase in the context of di-

rectionality reversal.

To understand the relation between $\alpha^{(d)}$ and $\alpha^{(-d)}$, we note the following symmetries of Λ . From Eq. (7), we see that replacing $d \rightarrow -d$, $A \rightarrow -A$, together with a complex conjugation, leaves Λ invariant, i.e. $\Lambda_{d \rightarrow -d, A \rightarrow -A} = \Lambda^*$. Using Eq. (8), this implies $\alpha^{(d)}(C, A, \theta) = \alpha^{(-d)}(C, -A, \theta)$ and $\bar{\chi}^{(d)}(C, A, \theta) = -\bar{\chi}^{(-d)}(C, -A, \theta)$. Consequently, the dephasing is only guaranteed to be symmetric ($\alpha^{(d)} = \alpha^{(-d)}$) when $A = 0$. Away from $A = 0$ there may be an additional antisymmetric component. We therefore denote A as the asymmetry parameter. Using the above symmetry relations, we write down the symmetric and antisymmetric dephasing components, $\alpha^{(d)} = \alpha^s + \alpha^a d$,

$$\alpha^s = \frac{1}{2} \left(\alpha^{(+1)}(C, A, \theta) + \alpha^{(+1)}(C, -A, \theta) \right), \quad (9)$$

$$\alpha^a = \frac{1}{2} \left(\alpha^{(+1)}(C, A, \theta) - \alpha^{(+1)}(C, -A, \theta) \right). \quad (10)$$

Next, defining a diagonal matrix $U = \text{diag}(1, -1, -1, 1)$, one shows that $\Lambda_{d \rightarrow -d, \theta \rightarrow \pi - \theta} = U \Lambda U$, which implies $\alpha^{(d)}(C, A, \theta) = \alpha^{(-d)}(C, A, \pi - \theta)$ and $\bar{\chi}^{(d)}(C, A, \theta) = \bar{\chi}^{(-d)}(C, A, \pi - \theta)$. This symmetry can

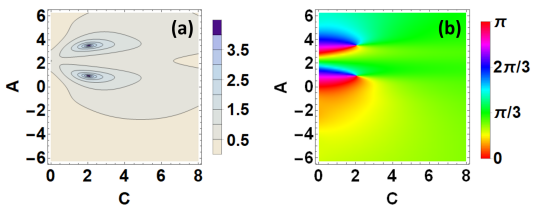


Figure 2. Dephasing $\alpha^{(+1)}$ (a) and phase $\bar{\chi}^{(+1)}$ (b), cf. Eq. (3), at $\theta = 3\pi/4$ color-coded as functions of the measurement strength (C) and asymmetry (A) parameters. Note the difference in behavior for $A > 0$ and $A < 0$, showing the effect of the measurement chirality. Most prominent are the two singularities at $C \approx 2$, where $\alpha^{(+1)}$ diverges. The phase makes π -windings around the points of divergent $\alpha^{(+1)}$.

be understood from a simple consideration: a clockwise ($d = -1$) protocol in the southern hemisphere becomes a counterclockwise ($d = 1$) protocol in the northern hemisphere upon exchanging the roles of the south and the north poles.

Asymmetric dephasing.—We next calculate numerically and analyze the behavior of $\alpha^{(+1)}$ (the behavior of $\alpha^{(-1)}$ can be inferred by swapping $\theta \rightarrow \pi - \theta$). Figure 2(a) shows the dependence of $\alpha^{(+1)}$ on the measurement parameters C and A at $\theta = 3\pi/4$. Note that $\alpha^{(+1)}(C, A, \theta) \neq \alpha^{(+1)}(C, -A, \theta) = \alpha^{(-1)}(C, A, \theta)$, revealing that the antisymmetric component α^a is indeed generically present as soon as $A \neq 0$ (i.e., whenever the measurements employed in the protocol possess chirality).

Note also the two divergences, $\alpha^{(+1)} \rightarrow \infty$, at $(C_{\text{crit}} \approx 2, A_{\text{crit}} > 0)$. There are no corresponding divergences at $A < 0$, implying that $\alpha^{(-1)}(C_{\text{crit}}, A_{\text{crit}}, \theta)$ is nonsingular. This implies that both $\alpha^a(C_{\text{crit}}, A_{\text{crit}}, \theta)$ and $\alpha^s(C_{\text{crit}}, A_{\text{crit}}, \theta)$ diverge. Moreover, the strength of divergence is identical as $\alpha^{(-1)} = \alpha^s - \alpha^a$ is finite. Contrast this to the case of dephasing in Hamiltonian-induced dynamics, where $\alpha^{(d)} = \beta\mathcal{E}T + \gamma d$ with $\mathcal{E}T \gg 1$ being the adiabaticity parameter (\mathcal{E} is the energy gap and T is the protocol execution time) [24, 25, 29]. There the symmetric component, $\alpha^s = \beta\mathcal{E}T$, associated with dynamical dephasing, always dominates over the antisymmetric geometrical dephasing $\alpha^a = \gamma d$ so that $\alpha^s/\alpha^a \sim \mathcal{E}T \gg 1$.

Divergences as topological features.—Consider the phase, $\bar{\chi}^{(+1)}(\theta = 3\pi/4)$, whose dependence on C and A is shown in Fig. 2(b). Remarkably, the phase makes a winding around each of the dephasing singularity points, cf. Fig. 2(a). Exactly at the singularity points, the phase is undefined since $e^{2i\bar{\chi}^{(+1)} - \alpha^{(+1)}} = 0$. The windings of the phase are of size π , and not 2π . However, since the measurable quantity is $e^{2i\bar{\chi}^{(+1)}}$, there is no physical discontinuity as $\bar{\chi}^{(+1)} \rightarrow \bar{\chi}^{(+1)} + \pi$. The windings cannot be eliminated by a continuous deformation of the phase, and thus constitute topological features. Such phase windings accompany all the divergences we found.

Another way of viewing the divergences as topological features arises when considering the set of all divergences. The divergences of $\alpha^{(+1)}$ form a critical line $(C_{\text{crit}}, A_{\text{crit}})$ in the (C, A) plane, cf. Figure 3. For each $(C_{\text{crit}}, A_{\text{crit}})$, there is a value of $\theta_{\text{crit}} \in [0; \pi]$ at which $\alpha^{(+1)}$ diverges. The critical line separates the plane into three regions. The θ -dependence of the phase $\bar{\chi}^{(+1)}(C, A, \theta)$ is topologically different in each of these regions. To see this, consider the dependence on the polar angle, θ , of $\bar{\chi}^{(+1)}(\theta)$ for a given value of measurement parameters (C, A) . For each given θ , $\bar{\chi}^{(+1)}$ is defined modulo π . However, taking the whole dependence on θ into account, we unfold the phase to form a continuous function $\bar{\chi}^{(+1)}(\theta)$ which is not confined to the interval $[0; \pi)$. Furthermore, note that $e^{2i\bar{\chi}^{(+1)}(\theta=0)} = e^{2i\bar{\chi}^{(+1)}(\theta=\pi)} = 1$. This implies

$$\bar{\chi}^{(+1)}(\pi) = \bar{\chi}^{(+1)}(\pi) - \bar{\chi}^{(+1)}(0) = \int_0^\pi d\theta \frac{d\bar{\chi}^{(+1)}(\theta)}{d\theta} = \pi\bar{n}, \quad (11)$$

where $\bar{n} \in \mathbb{Z}$ and we have used the freedom to fix $\bar{\chi}^{(+1)}(0) = 0$. No transition between different values of integer \bar{n} can happen when $\bar{\chi}^{(+1)}(\theta)$ is smoothly deformed, making \bar{n} a topological index. However, $\bar{n}(C, A)$ can jump when $\bar{\chi}^{(+1)}(\theta)$ is not a well-defined smooth function. This happens at the divergence points where $\alpha^{(d)}(C_{\text{crit}}, A_{\text{crit}}, \theta_{\text{crit}}) = +\infty$, so that $\bar{\chi}^{(+1)}(C_{\text{crit}}, A_{\text{crit}}, \theta_{\text{crit}})$ is undefined. Therefore, the (C, A) plane can be divided into regions, each with a distinct value of \bar{n} . In the present example, $\bar{n} = 0$ in region I , $\bar{n} = -1$ inside II , and $\bar{n} = -2$ inside III , as illustrated in Fig. 3(inset). The behavior of $\bar{\chi}^{(-1)}(\theta)$ is recovered via relation $\bar{\chi}^{(d)}(C, A, \theta) = \bar{\chi}^{(-d)}(C, A, \pi - \theta) \pmod{\pi}$, implying that for $d = -1$ similar topological transitions happen at the same $(C_{\text{crit}}, A_{\text{crit}})$ but at different θ_{crit} .

We emphasize the peculiarity of region II . Note that the phases $\chi_{\{r_k\}}^{(d)}$ corresponding to individual readout sequences are defined modulo 2π , cf. Eq. (4). Therefore, the behavior of regions I and III can be anticipated and observed for individual readout sequences [42]. However, no individual readout sequence allows for $\chi_{\{r_k\}}^{(d)}(\pi) - \chi_{\{r_k\}}^{(d)}(0) = \pm\pi$. Thus, the behavior of region II is a highly non-trivial consequence of averaging over multiple readout sequences in Eq. (3). This is reminiscent of the relation between the fields of dissipative topological matter [43–47] and measurement-induced entanglement transitions [48–60]. In the latter, looking at a refined observable that essentially depends on a non-trivial readout-averaging, gives rise to a number of new effects [61]. Furthermore, region II is only present when $A \neq 0$, showing that this behavior crucially depends on the measurement exhibiting chirality.

Summary.—We have presented here a protocol comprising a set of generalized measurements, which steers a spin-1/2 system along a closed trajectory on the Bloch sphere. Fluctuations in the readout sequences are responsible for dephasing, which is not symmetric under

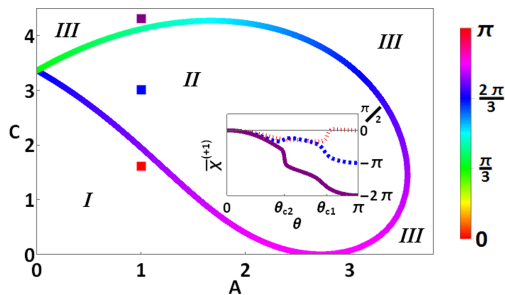


Figure 3. Topological transition in the measurement-induced phase $\bar{\chi}^{(+1)}$. Main panel—The critical line of points $(C_{\text{crit}}, A_{\text{crit}})$ for which there exists θ_{crit} such that the dephasing $\alpha^{(+1)}(C_{\text{crit}}, A_{\text{crit}}, \theta_{\text{crit}})$ diverges. The values of $\theta_{\text{crit}} \in [0; \pi]$ are shown with color. The averaged phase $\bar{\chi}^{(+1)}$ exhibits three distinctly different topological behaviors, corresponding to regions *I*, *II*, and *III*. Inset—Dependence of $\bar{\chi}^{(+1)}$ on θ for the measurement parameters (C, A) marked with squares in the main plot. As θ varies from 0 to π , $\bar{\chi}^{(+1)}(\theta)$ varies from 0 to 0 (region *I*), 0 to $-\pi$ (region *II*), or 0 to -2π (region *III*). The values of θ_{crit} corresponding to the two transitions at $A = 1$ are marked as θ_{c1} and θ_{c2} .

changing of path directionality, $d \rightarrow -d$. Rather it comprises two components: symmetric and antisymmetric. The latter is a manifestation of the measurement’s intrinsic chirality, a feature which, to the best of our knowledge, has not been previously emphasized.

The measurement-induced dynamics bears similitude to adiabatic Hamiltonian dynamics of open quantum systems, where symmetric (dynamical) and antisymmetric (geometrical) dephasing components have been predicted and observed [24–26, 29]. Indeed, the detector can be thought of as an external environment, while initializing the detector before each measurement amounts to Markovianity, often implied when describing open systems. At the same time, we find a number of important differences between these two paradigms of dephasing. For adiabatic Hamiltonian dynamics the identification of the symmetric and antisymmetric components with dynamical and geometrical dephasing respectively is clear-cut. This is not the case with measurement-induced dynamics. Furthermore, while in adiabatic Hamiltonian dynamics the antisymmetric component is always *much* smaller than the symmetric one, this does not apply for measurement-induced dephasing (nevertheless, the symmetric term always exceeds the antisymmetric term, which guarantees that for either directionality d the overall effect is suppression of coherent terms).

We have found divergences of the measurement-induced dephasing and linked them to topological transitions in the behavior of the measurement-induced phase factors. We note that a special case of such a transition ($A = 0$, cf. Eq. 2) has been discovered in Ref. [31]. We thus conclude that such transitions are a richer phenomenon than previously thought. This is revealed by

the corresponding “phase diagram”, cf. Fig. 3. In particular, region *II* in this phase diagram is only present for $A \neq 0$, i.e., for measurements that are chiral.

Finally, we stress that our findings extend beyond the concrete protocol and the specific type of measurements studied here. In particular, measurement-induced phases exhibit dephasing for an arbitrary number of measurements ($N < \infty$), arbitrary Kraus operators ($\mathcal{M}^{(r)}$), and arbitrary sequences of measurement directions (\mathbf{n}_k). The dephasing will, in general, be asymmetric w.r.t. reversal of the protocol directionality, and may diverge under certain conditions. For $N < \infty$, the dephasing and the induced phase will depend on N .

We thank V. Gebhart for useful discussions. We acknowledge funding by the Deutsche Forschungsgemeinschaft (DFG, German Research Foundation) – Projektnummer 277101999 – TRR 183 (project C01) and Projektnummern EG 96/13-1, GO 1405/6-1, and MI 658/10-2, and by the Israel Science Foundation (ISF).

-
- [1] D. Suter and G. A. Álvarez, Colloquium : Protecting quantum information against environmental noise, *Reviews of Modern Physics* **88**, 041001 (2016).
 - [2] A. Streltsov, G. Adesso, and M. B. Plenio, Colloquium : Quantum coherence as a resource, *Reviews of Modern Physics* **89**, 041003 (2017).
 - [3] Y. Imry, Introduction to mesoscopic physics (1997).
 - [4] A. Yacoby, U. Sivan, C. P. Umbach, and J. M. Hong, Interference and dephasing by electron-electron interaction on length scales shorter than the elastic mean free path, *Physical Review Letters* **66**, 1938 (1991).
 - [5] E. Shimshoni and A. Stern, Dephasing of interference in Landau-Zener transitions, *Physical Review B* **47**, 9523 (1993).
 - [6] F. Marquardt and D. S. Golubev, Relaxation and Dephasing in a Many-Fermion Generalization of the Caldeira-Leggett Model, *Physical Review Letters* **93**, 130404 (2004).
 - [7] A. Polkovnikov, K. Sengupta, A. Silva, and M. Vengalattore, Colloquium : Nonequilibrium dynamics of closed interacting quantum systems, *Reviews of Modern Physics* **83**, 863 (2011).
 - [8] O. Firstenberg, M. Shuker, A. Ron, and N. Davidson, Colloquium : Coherent diffusion of polaritons in atomic media, *Reviews of Modern Physics* **85**, 941 (2013).
 - [9] E. A. Laird, F. Kuemmeth, G. A. Steele, K. Grove-Rasmussen, J. Nygård, K. Flensberg, and L. P. Kouwenhoven, Quantum transport in carbon nanotubes, *Reviews of Modern Physics* **87**, 703 (2015).
 - [10] D. A. Abanin, E. Altman, I. Bloch, and M. Serbyn, Colloquium : Many-body localization, thermalization, and entanglement, *Reviews of Modern Physics* **91**, 021001 (2019), arXiv:1804.11065.
 - [11] A. A. Clerk, M. H. Devoret, S. M. Girvin, F. Marquardt, and R. J. Schoelkopf, Introduction to quantum noise, measurement, and amplification, *Reviews of Modern Physics* **82**, 1155 (2010).
 - [12] K. Hammerer, A. S. Sørensen, and E. S. Polzik, Quantum

- interface between light and atomic ensembles, *Reviews of Modern Physics* **82**, 1041 (2010).
- [13] Y. Makhlin, G. Schön, and A. Shnirman, Quantum-state engineering with Josephson-junction devices, *Reviews of Modern Physics* **73**, 357 (2001).
- [14] J. Gambetta, A. Blais, D. I. Schuster, A. Wallraff, L. Frunzio, J. Majer, M. H. Devoret, S. M. Girvin, and R. J. Schoelkopf, Qubit-photon interactions in a cavity: Measurement-induced dephasing and number splitting, *Physical Review A* **74**, 042318 (2006), arXiv:0602322 [cond-mat].
- [15] A. Frisk Kockum, L. Tornberg, and G. Johansson, Undoing measurement-induced dephasing in circuit QED, *Physical Review A* **85**, 052318 (2012), arXiv:1202.2386.
- [16] M. V. Berry, Quantal Phase Factors Accompanying Adiabatic Changes, *Proceedings of the Royal Society A: Mathematical, Physical and Engineering Sciences* **392**, 45 (1984).
- [17] E. Cohen, H. Larocque, F. Bouchard, F. Nejdastari, Y. Gefen, and E. Karimi, Geometric phase from Aharonov–Bohm to Pancharatnam–Berry and beyond, *Nature Reviews Physics* **1**, 437 (2019).
- [18] D. Ellinas, S. M. Barnett, and M. A. Dupertuis, Berry’s phase in optical resonance, *Physical Review A* **39**, 3228 (1989).
- [19] D. Gamliel and J. H. Freed, Berry’s geometrical phases in ESR in the presence of a stochastic process, *Physical Review A* **39**, 3238 (1989).
- [20] F. Gaitan, Berry’s phase in the presence of a stochastically evolving environment: A geometric mechanism for energy-level broadening, *Physical Review A* **58**, 1665 (1998).
- [21] J. E. Avron and A. Elgart, Adiabatic theorem without a gap condition: Two-level system coupled to quantized radiation field, *Physical Review A* **58**, 4300 (1998).
- [22] A. Carollo, I. Fuentes-Guridi, M. F. Santos, and V. Vedral, Geometric Phase in Open Systems, *Physical Review Letters* **90**, 160402 (2003).
- [23] G. De Chiara and G. M. Palma, Berry Phase for a Spin 1/2 Particle in a Classical Fluctuating Field, *Physical Review Letters* **91**, 090404 (2003).
- [24] R. S. Whitney and Y. Gefen, Berry Phase in a Nonisolated System, *Physical Review Letters* **90**, 190402 (2003).
- [25] R. S. Whitney, Y. Makhlin, A. Shnirman, and Y. Gefen, Geometric Nature of the Environment-Induced Berry Phase and Geometric Dephasing, *Physical Review Letters* **94**, 070407 (2005).
- [26] R. S. Whitney, Y. Makhlin, A. Shnirman, and Y. Gefen, Berry Phase with Environment: Classical versus Quantum, in *Theory of Quantum Transport in Metallic and Hybrid Nanostructures*, Vol. 230 (Kluwer Academic Publishers, Dordrecht, 2004) pp. 9–23, arXiv:0401376 [cond-mat].
- [27] K. Snizhko, R. Egger, and Y. Gefen, Non-Abelian Geometric Dephasing, *Physical Review Letters* **123**, 060405 (2019), arXiv:1904.11262.
- [28] K. Snizhko, R. Egger, and Y. Gefen, Non-Abelian Berry phase for open quantum systems: Topological protection versus geometric dephasing, *Physical Review B* **100**, 085303 (2019), arXiv:1904.11673.
- [29] S. Berger, M. Pechal, P. Kurpiers, A. A. Abdumalikov, C. Eichler, J. A. Mlynek, A. Shnirman, Y. Gefen, A. Wallraff, and S. Filipp, Measurement of geometric dephasing using a superconducting qubit, *Nature Communications* **6**, 8757 (2015).
- [30] Y.-W. Cho, Y. Kim, Y.-H. Choi, Y.-S. Kim, S.-W. Han, S.-Y. Lee, S. Moon, and Y.-H. Kim, Emergence of the geometric phase from quantum measurement back-action, *Nature Physics* , 1 (2019).
- [31] V. Gebhart, K. Snizhko, T. Wellens, A. Buchleitner, A. Romito, and Y. Gefen, Topological transition in measurement-induced geometric phases, *Proceedings of the National Academy of Sciences* **117**, 5706 (2020), arXiv:1905.01147.
- [32] Previously measurement-induced dephasing has been investigated in the context of superconducting qubits [14, 15]. We stress that there the dephasing was induced not by the measurement back-action but due to the ac Stark shift that appears in the physical implementation of the measurement process. Here we focus on the dephasing induced purely by the measurement back-action, assuming that the physical implementation does not add extra effects. Further, we emphasize that the dephasing considered in Refs. [14, 15] is due to a measurement in a fixed direction, and thus cannot pick up any geometric contribution.
- [33] In particular, the symmetry with respect to reversing the protocol is of interest. Naively, one expects measurement-induced dephasing to be symmetric. This is supported by the intuition of dealing with the Pancharatnam phase and of previous studies [31].
- [34] M. A. Nielsen and I. L. Chuang, *Quantum computation and quantum information* (Cambridge : Cambridge University Press, Cambridge, 2010).
- [35] H. M. Wiseman and G. J. Milburn, *Quantum measurement and control* (Cambridge University Press, 2010) p. 460.
- [36] K. Jacobs, *Quantum Measurement Theory and its Applications* (Cambridge University Press, Cambridge, 2014).
- [37] When tracing the detector out, i.e., treating it as an environment, this rotation would result in a Lamb shift, cf. Ref. [62].
- [38] P. Facchi, A. Klein, S. Pascazio, and L. Schulman, Berry phase from a quantum Zeno effect, *Physics Letters A* **257**, 232 (1999).
- [39] K. Snizhko, N. Rao, P. Kumar, and Y. Gefen, Weak-measurement-induced phases and dephasing: Broken symmetry of the geometric phase, *Physical Review Research* **3**, 043045 (2021), arXiv:2006.14641.
- [40] Y. Aharonov and J. Anandan, Phase change during a cyclic quantum evolution, *Physical Review Letters* **58**, 1593 (1987).
- [41] See also A. A. Wood, K. Streltsov, R. M. Goldblatt, M. B. Plenio, L. C. L. Hollenberg, R. E. Scholten, and A. M. Martin, Interplay between geometric and dynamic phases in a single-spin system, *Physical Review B* **102**, 125428 (2020), arXiv:2005.05619.
- [42] For more details see Ref. [39].
- [43] B. Kraus, H. P. Büchler, S. Diehl, A. Kantian, A. Micheli, and P. Zoller, Preparation of entangled states by quantum Markov processes, *Physical Review A* **78**, 042307 (2008).
- [44] H. Weimer, M. Müller, I. Lesanovsky, P. Zoller, and H. P. Büchler, A Rydberg quantum simulator, *Nature Physics* **6**, 382 (2010), arXiv:0907.1657.
- [45] S. Diehl, E. Rico, M. A. Baranov, and P. Zoller, Topology by dissipation in atomic quantum wires, *Nature Physics* **7**, 971 (2011).

- [46] L. Henriot, A. Scocchi, P. P. Orth, and K. Le Hur, Topology of a dissipative spin: Dynamical Chern number, bath-induced nonadiabaticity, and a quantum dynamo effect, *Physical Review B* **95**, 054307 (2017), [arXiv:1611.05085](#).
- [47] S. Roy, J. T. Chalker, I. V. Gornyi, and Y. Gefen, Measurement-induced steering of quantum systems, *Physical Review Research* **2**, 033347 (2020), [arXiv:1912.04292](#).
- [48] Y. Li, X. Chen, and M. P. A. Fisher, Quantum Zeno effect and the many-body entanglement transition, *Physical Review B* **98**, 205136 (2018), [arXiv:1808.06134](#).
- [49] A. Chan, R. M. Nandkishore, M. Pretko, and G. Smith, Unitary-projective entanglement dynamics, *Physical Review B* **99**, 224307 (2019), [arXiv:1808.05949](#).
- [50] B. Skinner, J. Ruhman, and A. Nahum, Measurement-Induced Phase Transitions in the Dynamics of Entanglement, *Physical Review X* **9**, 031009 (2019), [arXiv:1808.05953](#).
- [51] Y. Li, X. Chen, and M. P. A. Fisher, Measurement-driven entanglement transition in hybrid quantum circuits, *Physical Review B* **100**, 134306 (2019), [arXiv:1901.08092](#).
- [52] M. J. Gullans and D. A. Huse, Dynamical Purification Phase Transition Induced by Quantum Measurements, *Physical Review X* **10**, 041020 (2020), [arXiv:1905.05195](#).
- [53] X. Cao, A. Tilloy, and A. De Luca, Entanglement in a fermion chain under continuous monitoring, *SciPost Physics* **7**, 024 (2019), [arXiv:1804.04638](#).
- [54] M. Szyniszewski, A. Romito, and H. Schomerus, Entanglement transition from variable-strength weak measurements, *Physical Review B* **100**, 064204 (2019), [arXiv:1903.05452](#).
- [55] M. Szyniszewski, A. Romito, and H. Schomerus, Universality of Entanglement Transitions from Stroboscopic to Continuous Measurements, *Physical Review Letters* **125**, 210602 (2020), [arXiv:2005.01863](#).
- [56] Q. Tang and W. Zhu, Measurement-induced phase transition: A case study in the nonintegrable model by density-matrix renormalization group calculations, *Physical Review Research* **2**, 013022 (2020), [arXiv:1908.11253](#).
- [57] S. Choi, Y. Bao, X.-L. Qi, and E. Altman, Quantum Error Correction in Scrambling Dynamics and Measurement-Induced Phase Transition, *Physical Review Letters* **125**, 030505 (2020), [arXiv:1903.05124](#).
- [58] M. Ippoliti, M. J. Gullans, S. Gopalakrishnan, D. A. Huse, and V. Khemani, Entanglement Phase Transitions in Measurement-Only Dynamics, *Physical Review X* **11**, 011030 (2021), [arXiv:2004.09560](#).
- [59] Y. Li, X. Chen, A. W. W. Ludwig, and M. P. A. Fisher, Conformal invariance and quantum nonlocality in critical hybrid circuits, *Physical Review B* **104**, 104305 (2021), [arXiv:2003.12721](#).
- [60] M. Buchhold, Y. Minoguchi, A. Altland, and S. Diehl, Effective Theory for the Measurement-Induced Phase Transition of Dirac Fermions, [arXiv:2102.08381](#) (2021).
- [61] Y. Bao, S. Choi, and E. Altman, Symmetry enriched phases of quantum circuits, [arXiv:2102.09164](#) (2021).
- [62] F. Nathan and M. S. Rudner, Universal Lindblad equation for open quantum systems, *Physical Review B* **102**, 115109 (2020), [arXiv:2004.01469](#).